BIBECHANA
Vol. 23, No. 2, April 2026, 63-73

ISSN 2091-0762 (Print), 2382-5340 (Online)
Journal homepage: http://nepjol.info/index.php/BIBECHANA
Publisher:Dept. of Phys., Mahendra Morang A. M. Campus (Tribhuvan University)Biratnagar

Field assessment of corrosion probability in reinforced concrete structures using ASTM C876-based half-cell potential measurement in Tansen, Nepal

Madhab Gautam[1,2], Barsha Pandey[2], Shristi Paudel Chhetri[2], Lila Gaha[2], Nootan Prasad Bhattarai[1*], Jagadeesh Bhattarai[1]

[1]*Central Department of Chemistry, Tribhuvan University, Kirtipur, Kathmandu, Nepal.*
[2]*Department of Chemistry, Tribhuvan Multiple Campus, Tribhuvan University, Palpa, Nepal.*

*Corresponding authors: Email: neutan08@gmail.com

Abstract

The non–destructive, in–situ open-circuit potential mapping (OCPM) technique is used to investigate the corrosion probability conditions of rebar-embedded concretes (RECs) in urban areas of Tansen Municipality, Nepal. One hundred and three (103) REC samples of five different types are assessed in the present study. Corrosion condition of 51 building pillars (BPs), 27 reinforcement road slabs (R^2Ss), 10 building roofs (BRs), 10 fencing pillars (FPs), and 5 sewage supply pipes (S^2Ps) are evaluated from four surface points of each sample specimen per ASTM C876–22b standards. This assessment indicates the RECs of Tansen municipality areas are in a minimal or least corrosion risk (LCR) zone, i.e., <10 % probability of corrosion. RECs with rough-cracked surfaces in high humidity show a zone of severe corrosion risk per the recorded OCP values. The REC pillars of the buildings are at a slightly higher corrosion risk than the building roof slabs. Reinforcing rebars of S^2Ps and FPs with low or negative open circuit potential values are more vulnerable than BRs and R^2Ss of Tansen.

Keywords
Corrosion potential, corrosion assessment, embedded rebar, open circuit potential, reinforced concrete.

Article information
Manuscript received: November 22, 2025; Revised: April 17, 2026; Accepted: April 26, 2026
DOI: https://doi.org/10.3126/bibechana.v23i2.86768

1 Introduction

Concrete is one of the construction materials in the construction industry, primarily due to its high compressive strength, sustainability, and versatility [1]. Nevertheless, its inherently low tensile strength necessitates the embedded of steel reinforcement bars to ensure structural integrity of concrete [2]. Thus, the form composite system is called rebar-embedded concrete (REC), which underpins essential infrastructure such as building pillars, roofs, beams, bridges, flyovers, and dams [3].

However, the reinforced concrete structure can deteriorate due to corrosion of the reinforcing steel. The formation of rust on the reinforcing metal is enhanced when environmental pollutants, chlorides, carbon dioxide, sulphates, etc., ingress into reinforced concrete. Rust on reinforcing steel leads to volumetric expansion (two to six times), inducing stresses that cause spalling and cracking, ultimately reducing structural durability [4].

Various approaches are adopted to prevent the corrosion of embedding rebar (ER) in concrete. Cathodic protection methods utilizing impressed current or sacrificial anodes can use that retards electrochemical processes, whereas anode is made passive with anodic protection techniques [5]. Galvanization and electroplating techniques as surface treatment strategies to promote the anti-corrosion activity of ER in the concrete system. These days, more than 25 gigatonnes of concrete are used annually as construction materials in ERC. But ERC corrosion is a big challenge for developing countries like Nepal [6]. Various aging structures in Nepal, constructed before the adoption of modern design standards or codes such as NBC 105:2020, suffer from inadequate durability [7], leaving them highly susceptible to corrosion-related deterioration [8]. The corrosion mechanism of ER involves oxidizing iron-based materials at anodic sites, where electrons transfer to cathodic regions; consequently, ferrous ions form at the anode. These ferrous ions, combined with hydroxide ions from moisture in aerated conditions, produce voluminous hydrated ferric oxide (rust), which creates internal tensile stresses, causing ERC to spall, crack, and undergo corrosive degradation of the ER service life over time [9, 10].

An open circuit potential mapping (OCPM) technique is *an in-situ* in-situ and non-destructive electrochemical procedure that is applied to investigate the ER corrosion in ERC [11]. The OCPM method, in accordance with ASTM C876-22b protocol, is applicable for probabilistic predictions of corrosion status of reinforced steel bars in concrete [12]. This method, however, is a qualitative method for preliminary corrosion assessments, which is applicable for predicting the corrosion condition of REC structures [13]. The measurement of open-circuit potential (OCP) is a sensitive factor in the OCPM technique [14]. It depends on the surrounding conditions (such as moisture, chloride, sulfate, CO_2 availability, and conductivity) of the concrete structures [15].

Evaluation of corrosion risks has been carried out in areas of Nepal such as the Pokhara Valley [7], the Kathmandu Valley [13], and sub-metropolises of Butwal [6] and Bhairahawa [16]; however, areas like Tansen municipality, which are undergoing significant urban growth with increased industrial sectors (cement and crusher industry in Palpa, 14 pharmaceutical industries in Rupandehi) and increased environmental exposure, have been largely overlooked. This research aims to address a gap by applying the OCPM technique to recorded OCP values from the resisting elements of the reinforced concrete building's pillars and roofs, reinforcement road slabs, fencing pillars, and sewage supply pipes in Tansen city areas. The study highlights the identification of the severity, progression, and underlying factors contributing to reinforced concrete corrosion. Therefore, the present research work is aimed to conduct preliminary and non-destructive assessment of corrosion probability using ASTM C876-22b standard OPCM technique. Also, corrosion probability of selected concrete infrastructures is compared and baseline data for future detailed studies is provided. The previous study recommended tailoring maintenance and retrofitting of these rebar-embedded concrete (REC) structures [17]. The findings also enriched current knowledge for designing REC materials to extend their durability and resilience in urban cities of Nepal.

2 Materials and methods

To forecast the corrosion risk probability of the 103 REC foundations, such as 51 building pillars (BPs), 27 reinforced road slabs (R^2Ss), 10 building roofs (BRs), 10 fencing pillars (FPs), and 5 sewage supply pipes (S^2Ps), available in the Tansen city areas of Nepal were selected in accordance with purposive sampling methods (Figure 1), were meticulously assessed by recording their open circuit potential (OCP) values using the potential mapping method per ASTM C876-22b standard [12], after a careful visual inspection of the sample specimens' morphological and physical characteristics. The OCP from four points of each sample specimens was recorded to quantify three possible corrosion risk zones using a digital voltmeter, which was connected with a saturated calomel electrode (SCE) serving as the reference electrode and the embedded rebar (ER) as the working electrode. The reference electrode was placed on the surface of the REC foundations with the help of a wetted sponge (Figure 2), as described elsewhere [18]. The OCP from these selected samples was measured within two weeks (2^{nd} and 3^{rd} week of January) and the ambient temperature and humidity were 16±7 °C and 39±3 %, respectively.

The OCPM technique is employed to assess the corrosion possibility of RECs. This technique classifies the likelihood of active or passive corrosion labels based on average OCP values [19], Table 1.

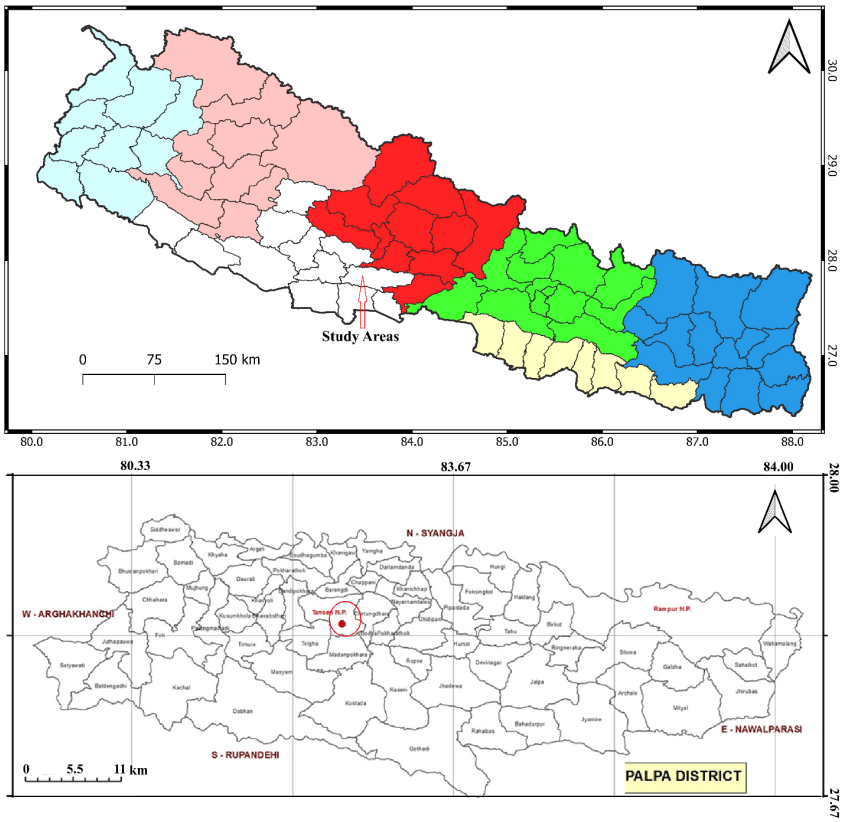

Figure 1: Map of showing selected samples of building pillars, road slabs, building roofs, fencing pillars, and sewage pipes available in Tansen municipal urban areas.

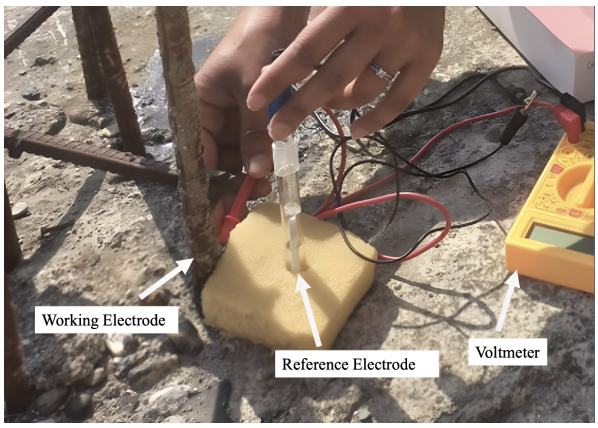

Figure 2: Set up utilizing for HCP measurements for predicting risk of RSC in the samples available around urban municipal areas of Tansen.

An OCP value nobler than −126 mV vs SCE corresponds to the least corrosion risk (LCR), with a corrosion probability of less than 10% (Table 1). The OCP value between −126 mV and −276 mV indicates mid corrosion risk (MCR); a definitive conclusion is not possible [12]. Furthermore, an OCP value < -276 mV indicates a severe corrosion risk (SCR) with a corrosion likelihood exceeding 90%. Using this protocol, all one hundred and three (103) RECs were evaluated, which are available in the urban areas of Tansen municipality. The results classify each sample into one of three levels of corrosion risk: LCR, MCR, and SCR. This categorization will provide a foundation for understanding corrosion severity, helping to direct future maintenance strategies and durability examinations for RECs.

Table 1: Qualitative evaluation of corrosion risk probability of ERC infrastructures, dependent on the average OCP value [12]

Mean OCP (mV vs SCE)	Corrosion Risk level of ERCs
> -126	Least or (<10%) corrosion risk (LCR)
$-276 < x < -126$	Mildly or (10-90%) corrosion risk (MCR)
< -276	Severely or (>90%) corrosion risk (SCR)

3 Results and discussion

Tables 2, 3, 4, 5 and 6 provide a comprehensive overview of the physical and morphological properties of the 103 RECs, as well as their average OCP values. Table 2 shows the summary of the physical morphological properties of all 51–building pillar (BP) samples. Among the fifty-one (51) building pillar (BP) samples (Table 2), the majority (82.3%

or 42 samples) were classified as being in a minimal or negligible corrosion risk (LCR), with less than 10% probability of corrosion, based on the mean OCP values more positive than –126 mV (SCE). In contrast, six samples (11.8%) of the BPs indicated a mildly-corrosion risk (MCR), corresponding to a 10—90% probability of corrosion with the mean OCP between −126 and −275 mV (SCE). Only three BP samples (5.9%) are in an active corrosion state or severe corrosion risk, with mean OCP values more negative than ˇ276 mV (SCE), as illustrated in Figure 3.

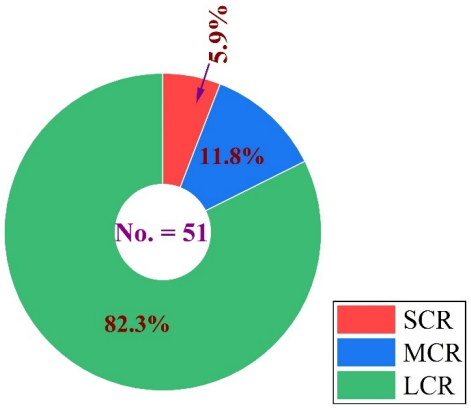

Figure 3: Pie chart showing the distribution of three corrosion probability zones of the building pillars of the study areas.

These outcomes demonstrate that most pillars in the investigated sites of urban Tansen municipal areas retain their load-bearing capacity; this is largely attributable to the lack of active corrosion or SCR (only 5.9%), which prevents the reinforcement–concrete bond established during construction. Minor repairs could extend the service life of the buildings, according to OCP values. Building pillars are critical reinforced concrete structures because they deliver resilience by bearing the load of the structure and preventing it from corrosive damage [20], distributing the burden of the whole structure by evenly transferring the resisting force from the upper parts of the building to the foundation [21,22].

The corrosion conditions of twenty-seven reinforced road slabs (R^2Ss), collected from the study area, were evaluated using recorded OCP values. Among these, only one R^2S sample, designated as R^2S–26, representing an older road slab, was identified as being highly susceptible to severe or active corrosion (SCR), with a corrosion probability exceeding 90%. Additionally, eight road slabs, accounting for 29.6%, were categorized as moderately corroded (MCR), based on average potential values recorded between -141.8 ± 1.3 mV and -210.0 ± 2.09 mV (SCE). Furthermore, 66.7% of the R^2S samples are assumed to be slightly corroded, indicating a corrosion probability of less than 10%, as illustrated in Table 3 and Figure 4. Overall, these findings suggest that the reinforced road slab (R^2S) specimens are comparatively less vulnerable to corrosion of reinforcing mild steel in concrete infrastructures.

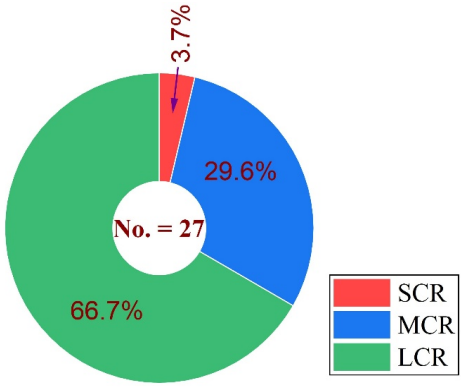

Figure 4: Pie chart showing the distribution of three corrosion probability zones of the reinforced road slab (R^2S) samples of the study areas.

It is meaningful to mention herein that corrosion of reinforcing rebars in concrete roads is caused by chloride ions, carbonation, and climate change, which are concerns during their service life [23]. The chloride- and carbocation–induced concrete corrosion in Tansen city is likely minimal. It is situated in a hilly region and has no industries that emit pollutant gases, and is far from the marine environment, such as the sea [24]. Roads in the study areas do not freeze during winter, so ice-melting chloride salts, which are harmful to reinforced concrete, are not used in Tansen city areas, making them less susceptible to the types of reinforced concrete road corrosion associated with these agents. Of course, the humidity, annual temperature, moisture, and drainage system also affect the corrosion of reinforcing rebar in reinforced concrete [25]. Therefore, the possible mechanisms of corrosive deterioration in these R^2Ss may involve environmental changes that generate rust and expansive pressure, leading to cracking and spalling of the most concrete cover of these samples, as illustrated in Table 3.

Table 4 shows the summary of the physical and morphological properties of 10-building roof (BR) samples. Among these BR samples, the most of them (i.e., 9 out of 10 or 90%) are in the least corrosion risk (LRC) zone with more noble potential than -126 mV (SCE) values, except one old sample (BR-10) with -163.25 ±1.26 mV (SCE), which is assumed to exist in the MCR zone, with a corrosion possibility ranging from 10% to 90%, as illustrated in Figure 5.

Table 2: Condition of the building pillar (BP) samples of Tansen city areas, based on the mean OCP values, including their physico–morphological properties

Sample code	Physico-morphological properties of BuP samples	OCP (mV vs SCE)		Corrosion condition
		Mean (n=4)	SD	
BP-1	Aged, dry, rough surface, no (cracking-spalling-rust stains)	−76.00	±1.37	LCR
BP-2	New, wet, rough surface, no (cracking-spalling-rust stains)	−82.50	±3.24	LCR
BP-3	Aged, dry, rough surface, no (cracking-spalling-rust stains)	−57.25	±1.48	LCR
BP-4	Aged, dry, smooth surface, no (cracking-spalling-rust stains)	−64.75	±1.48	LCR
BP-5	New, dry, smooth surface, no (cracking-spalling-rust stains)	−69.01	±3.75	LCR
BP-6	Aged, dry, rough surface, no (cracking-spalling-rust stains)	−57.75	±1.48	LCR
BP-7	Aged, dry, smooth surface, no (cracking-spalling-rust stains)	−28.75	±4.55	LCR
BP-8	Aged, dry, smooth surface, no (cracking-spalling-rust stains)	−92.01	±6.78	LCR
BP-9	Aged, dry, rough surface, cracking-spalling-rust stains	−328.80	±3.74	SCR
BP-10	New, dry, smooth surface, no (cracking-spalling-rust stains)	−15.02	±3.39	LCR
BP-11	New, dry, smooth surface, no (cracking-spalling), light stains	−90.75	±3.96	LCR
BP-12	Aged, dry, smooth surface, cracking-spalling, light rust stains	−105.25	±5.26	LCR
BP-13	Aged, dry, smooth surface, no (cracking-spalling), light rust stains	−115.50	±6.98	LCR
BP-14	New, dry, smooth surface, no (cracking-spalling), light rust stains	−89.50	±7.66	LCR
BP-15	Aged, dry, rough surface, cracking-spalling, light rust stains	−120.01	±1.87	LCR
BP-16	Aged, dry, rough surface, cracking-spalling; light rust stains	−165.25	±6.18	MCR
BP-17	Aged, dry, smooth surface, no (cracking-spalling), light rust stains	−112.25	±4.60	LCR
BP-18	New, dry, smooth surface, no (cracking-spalling), light rust stains	−120.01	±4.95	LCR
BP-19	New, dry, smooth surface, no (cracking-spalling), light rust stains	−104.01	±4.24	LCR
BP-20	Aged, dry, smooth surface, no (cracking-spalling-rust stains)	−73.01	±4.64	LCR
BP-21	New, dry, smooth surface, no (cracking-spalling-rust stains)	−93.50	±5.32	LCR
BP-22	Aged, dry, smooth surface, cracking-spalling, no rust stains	−80.25	±3.03	LCR
BP-23	Aged, dry, smooth surface, no (cracking-spalling-rust stains)	−88.25	±6.18	LCR
BP-24	New, dry, smooth surface, no (cracking-spalling-rust stains)	−104.50	±5.77	LCR
BP-25	New, dry, smooth surface, no (cracking-spalling-rust stains)	−95.75	±5.54	LCR
BP-26	Aged, dry, smooth surface, no (cracking-spalling-rust stains)	−81.75	±4.66	LCR
BP-27	Aged, dry, smooth surface, no (cracking-spalling), light rust stains	−129.50	±5.85	MCR
BP-28	Aged, dry, rough surface, no (cracking-spalling-rust stains)	−76.50	±6.18	LCR
BP-29	Aged, dry, smooth surface, no (cracking-spalling-rust stains)	−82.50	±6.18	LCR
BP-30	New, dry, smooth surface, no (cracking-spalling), light rust stains	−121.25	±5.31	LCR
BP-31	New, dry, smooth surface, no (cracking-spalling-rust stains)	−91.50	±4.39	LCR
BP-32	New, dry, smooth surface, no (cracking-spalling-rust stains)	−95.01	±5.61	LCR
BP-33	New, dry; smooth surface; no cracking and spalling; no rust stains	−72.75	±4.32	LCR
BP-34	New, dry; smooth surface; no (cracking-spalling-rust stains)	−80.75	±6.18	LCR
BP-35	Aged, dry, rough surface, no (cracking-spalling), light rust stains	−115.01	±6.20	LCR
BP-36	New, dry, smooth surface, no (cracking-spalling-rust stains)	−97.50	±6.10	LCR
BP-37	New, dry, smooth surface, no (cracking-spalling-rust stains)	−5.33	±1.52	LCR
BP-38	Aged, wet, rough surface, no (cracking-spalling-rust stains)	−121.35	±1.29	LCR
BP-39	New, dry, smooth surface, no (cracking-spalling- rust stains)	−45.01	±2.44	LCR
BP-40	Aged, dry, smooth surface, no (cracking-spalling-rust stains)	−3.75	±0.13	LCR
BP-41	New, dry, smooth surface, no (cracking-spalling-rust stains)	−2.25	±0.95	LCR
BP-42	Aged, dry, smooth surface, no (cracking-spalling-rust stains)	−12.10	±2.53	LCR
BP-43	Aged, dry, smooth surface, no (cracking-spalling-rust stains)	−3.35	±0.53	LCR
BP-44	Aged, dry, rough surface, no (cracking- spalling), light rust stains	−122.13	±0.84	LCR
BP-45	Aged, dry, rough surface, no (cracking- spalling), rust stains	−194.25	±4.11	MCR
BP-46	Aged, dry, rough surface, no (cracking- spalling), rust stains	−282.50	±2.03	SCR
BP-47	Aged, dry, rough surface, no (cracking- spalling), rust stains	−166.50	±3.05	MCR
BP-48	Aged, wet, rough surface, no (cracking- spalling), rust stains	−152.75	±1.04	MCR
BP-49	Aged, dry, smooth surface, no (cracking-spalling-rust stains)	−40.73	±2.71	LCR
BP-50	Aged, dry, rough surface, cracking and spalling, rust stains	−327.12	±1.19	SCR
BP-51	Aged, dry, rough surface, cracking and spalling, rust stains	−205.25	±2.45	MCR

Table 3: Corrosion condition of the reinforced road slab (R^2S) samples of Tansen city areas based on mean OCP values and physico-morphological properties

Sample Code	Physico-morphological Properties	OCP (mV vs SCE)		Condition
		Mean (n=4)	SD	
R^2S-1	Aged, dry, rough surface, cracking & spalling, rust stains	−141.75	±1.30	MCR
R^2S-2	Aged, dry, rough surface, cracking & spalling, rust stains	−121.00	±1.22	LCR
R^2S-3	Aged, wet, rough surface, cracking & spalling, rust stains	−149.50	±3.20	MCR
R^2S-4	Aged, dry, smooth surface, cracking & spalling, rust stains	−113.75	±1.92	LCR
R^2S-5	Aged, dry, rough surface, cracking & spalling, rust stains	−168.50	±3.64	MCR
R^2S-6	Aged, dry, rough surface, no (cracking & spalling), rust stains	−111.50	±4.22	LCR
R^2S-7	Aged, dry, rough surface, cracking & spalling, rust stains	−150.50	±1.54	MCR
R^2S-8	Aged, dry, smooth surface, no (cracking, spalling & rust stains)	−82.75	±3.56	LCR
R^2S-9	Aged, dry, rough surface, no (cracking, spalling & rust stains)	−97.00	±4.30	LCR
R^2S-10	Aged, dry, rough surface, cracking & spalling, rust stains	−118.25	±3.90	LCR
R^2S-11	Aged, dry, rough surface, cracking & spalling, no rust stains	−100.75	±3.79	LCR
R^2S-12	Aged, dry, rough surface, cracking & spalling, rust stains	−168.50	±2.56	MCR
R^2S-13	Aged, dry, rough surface, cracking & spalling, rust stains	−120.00	±1.87	LCR
R^2S-14	Aged, dry, rough surface, no (cracking, spalling & rust stains)	−71.50	±3.37	LCR
R^2S-15	Aged, dry, rough surface, cracking & spalling, rust stains	−130.50	±2.18	MCR
R^2S-16	Aged, dry, smooth surface, no (cracking, spalling & rust stains)	−83.25	±4.44	LCR
R^2S-17	Aged, dry, smooth surface, no (cracking, spalling & rust stains)	−81.25	±2.58	LCR
R^2S-18	Aged, dry, smooth surface, no (cracking, spalling & rust stains)	−73.00	±3.64	LCR
R^2S-19	Aged, dry, rough surface, no (cracking, spalling & rust stains)	−72.25	±3.34	LCR
R^2S-20	Aged, dry, smooth surface, no (cracking, spalling & rust stains)	−80.50	±3.64	LCR
R^2S-21	Aged, dry, rough surface, no (cracking, spalling & rust stains)	−68.75	±1.71	LCR
R^2S-22	Aged, dry, rough surface, no (cracking, spalling & rust stains)	−67.75	±3.56	LCR
R^2S-23	Aged, dry, rough surface, no (cracking, spalling & rust stains)	−109.50	±2.81	LCR
R^2S-24	Aged, wet, rough surface, cracking & spalling, rust staining	−210.00	±2.09	MCR
R^2S-25	Aged, wet, smooth surface, cracking & spalling, rust stains	−146.00	±2.39	MCR
R^2S-26	Aged, wet, rough surface, cracking & spalling, rust stains	−327.50	±2.39	SCR
R^2S-27	Aged, dry, smooth surface, no (cracking, spalling & rust stains)	−79.00	±3.48	LCR

Table 4: Corrosion condition of the building roof (BR) samples of Tansen city areas based on mean OCP values and physico–morphological properties

Sample No.	Physico-morphological Properties of BR Specimens	OCP (mV vs SCE)		Condition
		Mean (n=4)	SD	
BR-1	New, dry, rough surface, no (cracking, spalling & rust stains)	−63.80	±3.79	LCR
BR-2	Aged, dry, rough surface, no (cracking, spalling & rust stains)	−72.80	±1.95	LCR
BR-3	New, dry, smooth surface, no (cracking, spalling & rust stains)	−125.00	±2.24	LCR
BR-4	New, dry, smooth surface, no (cracking, spalling & rust stains)	−103.00	±2.71	LCR
BR-5	New, dry, smooth surface, no (cracking, spalling & rust stains)	−63.75	±2.86	LCR
BR-6	New, dry, smooth surface, no (cracking, spalling & rust stains)	−18.40	±1.84	LCR
BR-7	New, dry, rough surface, no (cracking, spalling & rust stains)	−77.00	±3.18	LCR
BR-8	New, dry, smooth surface, no (cracking, spalling & rust stains)	−3.75	±0.13	LCR
BR-9	Aged, dry, smooth surface, no (cracking, spalling & rust stains)	−23.50	±0.68	LCR
BR-10	Aged, dry, rough surface, no (cracking & spalling), rust stains	−163.25	±1.26	MCR

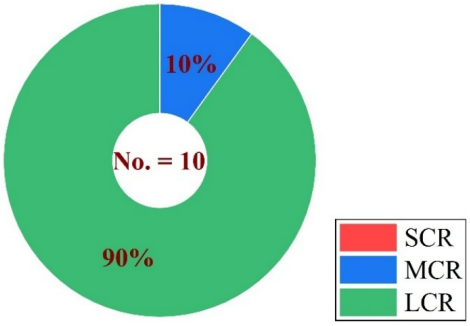

Figure 5: Pie chart showing the distribution of three corrosion probability zones of the building roofs (BRs) of the study areas.

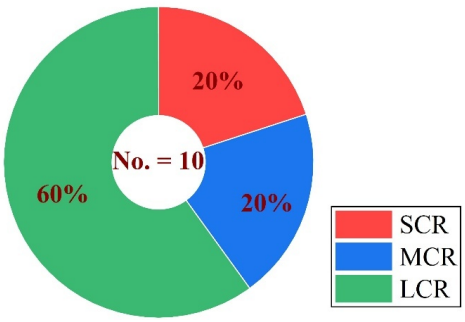

Figure 6: Pie chart showing the distribution of three corrosion probability zones of the fencing pillars of the study areas.

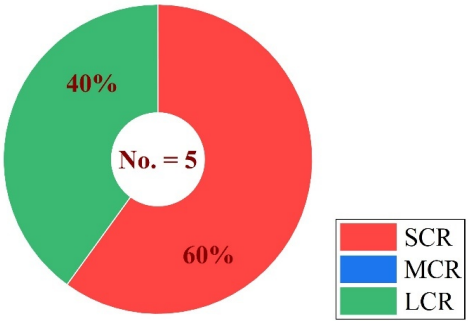

Figure 7: Pie chart showing the distribution of three corrosion probability zones of the sewage supply pipes of the study areas.

Comprehending the essential causes of BR corrosive degradation, such as a high water–to–cement ratio, qualityless materials, increased permeability, and inadequate curing process, makes it more susceptible to corrosion [26]. In addition, structures exposed to corrosive elements such as chloride, CO_2, or extreme weather conditions can also be more vulnerable [27]. The present study areas of Tansen city are assumed to be free of atmospheric pollutants, like chloride and CO_2, as discussed above. Therefore, most residential building roof samples appear safe from corrosive degradation in the ambient environment of Tansen city.

Furthermore, among the ten-fencing pillar (FP) samples of Tansen city areas, 60% (six samples)

were classified as least corrosion risk (LCR), 20% of the samples (two samples) ranked to be mildly corrosion risk (MCR), and the remaining 20% (FP-1 & FP-2) are vulnerable to corrosion, as shown in Table 5 and Figure 6. Similarly, 60% of the sewage supply pipe (S^2P) samples (three out of five) exhibited severe corrosion risk (SCR), as illustrated in Table 6 and also in Figure 7.

The analyzed OCP data clearly indicate that the FPs and S^2Ps in the Tansen city areas are the most prone to corrosion, with 20–60% of samples showing signs of active corrosion. These results highlight the impact of environmental conditions on the rebar within concrete infrastructures, consistent with previous reports [28, 29]. In contrast, components of residential buildings, such as roofs and pillars, demonstrate a significant level of durability and a very low risk of deterioration. Findings align with the previously reported research [7, 15, 16]. Their studies support the conclusion that this approach is effective in predicting structural integrity and assessing potential corrosion risks.

Table 5: Corrosion condition of the fencing pillar (FP) samples of Tansen city areas based on mean OCP values and physico–morphological properties

Sample No.	Physico-morphological Properties of FP Specimens	OCP (mV vs SCE)		Condition
		Mean (n=4)	SD	
FP-1	Aged, dry, rough surface, cracking & spalling, rust stains	−351.00	±1.37	SCR
FP-2	Aged, wet, rough surface, cracking & spalling, rust stains	−378.00	±1.91	SCR
FP-3	Aged, dry, rough surface, cracking & spalling, rust stains	−115.00	±2.91	LCR
FP-4	Aged, dry, rough surface, cracking & spalling, rust stains	−127.00	±3.08	MCR
FP-5	Aged, dry, rough surface, no (cracking & spalling), rust stains	−123.00	±1.21	LCR
FP-6	Aged, dry, smooth surface, no (cracking, spalling & rust stains)	−21.58	±0.21	LCR
FP-7	Aged, dry, smooth surface, cracking & spalling, no rust stains	−129.00	±3.48	MCR
FP-8	Aged, dry, rough surface, no (cracking, spalling & rust stains)	−34.99	±0.18	LCR
FP-9	Aged, wet, rough surface, no (cracking, spalling & rust stains)	−20.41	±0.08	LCR
FP-10	Aged, dry, rough surface, cracking & spalling, light rust stains	−28.25	±9.14	LCR

Table 6: Condition of the sewage supply pipe (S^2P) samples of Tansen city areas, based on the mean OCP values, including their physico–morphological properties

Sample No.	Physico-morphological Properties of FP Specimens	Mean (n=4)	SD	Corrosion Condition
S2P-1	New, dry, rough surface, cracking & spalling, rust stains	-419.00	± 4.18	SCR
S2P-2	Aged, wet, rough surface, cracking & spalling, rust stains	-358.00	± 2.56	SCR
S2P-3	Aged, dry, rough surface, cracking & spalling, rust stains	-435.00	± 1.61	SCR
S2P-4	New, dry, smooth surface, cracking & spalling, no rust stains	-27.80	± 1.05	LCR
S2P-5	Aged, dry, smooth surface, cracking & spalling, light rust stains	-23.75	± 0.83	LCR

3.1 Conclusion

A study of one hundred and three (103) steel rebar–embedded concrete (REC) infrastructures in Tansen municipality areas using the in-situ OCP mapping (OCPM) method aligned with ASTM C876–22b protocols, identified key differences in corrosion risk probability of embedding steel (ES) rebar. Sewage pipes and fencing pillars were the most vulnerable, with many showing a severe to mild risk of corrosion probability, suggesting they need immediate attention. Conversely, building pillars and roofs for residential purposes available in investigated urban city areas were found to be highly durable or with minimal corrosion risks, showing little to no signs of corrosion. These conclusions are listed below point-wise:

- Residential building pillars, concrete roofs, and reinforcement road slabs are at low risk for corrosion (mean OCP>-126 mv vs SCE), demonstrating high durability with few signs of corrosion.
- Fencing pillars (FP) indicate varying corrosion risk levels, categorized mainly as having a mild probability of corrosion (mean OCP is between -276 mv vs SCE and -126 mv vs SCE).
- The sewage supply pipes (S^2Ps) of the study areas have a comparatively high probability of corrosion (mean OCP<-276 mv vs SCE), indicating a mostly moderate corrosion risk level (MCR).
- Structures located in damp environments, like sewage supply pipes, are more susceptible to corrosion compared to those in drier conditions.
- The examination reveals that environmental factors, such as high humidity and exposure to water, are significant contributors to corrosion risk.

Acknowledgments

The authors thank to local people for their assistance in sampling the concrete species and to Department of Chemistry, Tribhuvan Multiple Campus, Tansen for providing research opportunity and facilities.

Author contributions

NPB and JB planned the experiments; specimen selection and preparation, data recorded and examination by MG, BP, SPC, and LG; interpreted the data and outcomes overview by NPB and JB; wrote the manuscript draft by MG and NPB; and edited and finalized by NPB and JB. All authors read and consented to the final manuscript.

Conflict of interest

The authors proclaim that they hold no conflicts of interest

Data availability statement

Upon demand, the corresponding author(s) will supply data to reinforce their conclusions.

References

[1] Nilimaa J. Smart materials and technologies for sustainable concrete construction. Developments in the Built Environment. 2023;15:100177.

[2] Gautam M, Bhattarai NP, Bhattarai J. Sesamum indicum leaf extract as environmentally benign inhibitor to mitigate mild steel corrosion in cement pore solution. Journal of Institute of Science and Technology. 2025;30(1):101-13.

[3] Firoozi AA, Firoozi AS, Oyejobi DO, Avudaiappan S, Flores ES. Emerging trends in sustainable building materials: technological innovations, enhanced performance, and future directions. Results in Engineering. 2024;24:103521.

[4] Ali M, Shams MA, Bheel N, Almaliki AH, Mahmoud AS, Dodo YA, et al. A review on chloride induced corrosion in reinforced concrete structures: Lab and in situ investigation. RSC Advances. 2024;14(50):37252-71.

[5] Yahaya MS, Kumar D, Nahar K, Usman HM, Gambo AS, Aminu T, et al. Advancements in anode materials for cathodic protection: nanostructured alloys, surface modifications, and smart monitoring. Buletin Ilmiah Sarjana Teknik Elektro. 2024;6(3):281-307.

[6] Magar KTK, Paudel Y, Gautam M, Bhattarai NP, Bhattarai J. Durability judgment of reinforced concrete infrastructures around Butwal sub-metropolitan city areas with corrosion potential mapping method. Journal of Nepal Chemical Society. 2024;45(2):147-56.

[7] Laudari I, Phulara NR, Gautam M, Bhattarai J. Evaluation of corrosion condition of some steel-reinforced concrete infrastructures avail-

able in Pokhara Valley of Nepal. Tribhuvan University Journal. 2021;36(01):1-17.

[8] Shrestha J, Lamichhane A, Giri B, Koirala BR, Paudel N. Impact of revised code NBC105 on assessment and design of low rise reinforced concrete buildings in Nepal. Journal of Institute of Engineering. 2021;16(1):1-5.

[9] Mahi MSH, Ridoy TA, Sarder AA. Corrosion mechanisms in reinforced concrete: causes, effects, and sustainable mitigation strategies. Current Problems in Research. 2025;1:52-66.

[10] Bhattarai J. Frontiers of Corrosion Science. 1st ed. Kathmandu, Nepal: Kshitiz Publication; 2010.

[11] Gautam M, Subedi DB, Dhungana JR, Bhattarai NP, Bhattarai J. Utilization of bark extract of Phyllanthus emblica as a sustainable corrosion inhibitor to reinforced concrete infrastructures in aggressive environments. In: E3S Web of Conferences. vol. 610; 2025. p. 03002.

[12] ASTM C876-22b. Standard Test Method for Corrosion Potentials of Uncoated Reinforcing Steel in Concrete. West Conshohocken, PA, USA: ASTM International; 2022.

[13] Phulara NR, Bhattarai J. Assessment on corrosion damage of steel-reinforced concrete structures of Kathmandu Valley using corrosion potential mapping method. Journal of Institute of Engineering. 2019;15(2):47-56.

[14] Gautam M, Subedi DB, Dhungana JR, Dhakal M, Bohara KP, Bhattarai NP, et al. A sustainable approach for mitigating rebar corrosion in adverse conditions using Phyllanthus emblica (L.) leaf extract as concrete scale inhibitor. International Journal of Corrosion and Scale Inhibitor. 2025;14(3):1522-54.

[15] Figueira RB. Electrochemical sensors for monitoring the corrosion conditions of reinforced concrete structures: A review. Applied Sciences. 2017;7(11):1157.

[16] Magar KTK, Paudel Y, Gautam M, Bhattarai NP, Bhattarai J. Predictive evaluation on corrosion impacts of reinforcement concrete infrastructures available in Bhairahawa city areas with half-cell potential measurement. Amrit Research Journal. 2025;6(1):26-35.

[17] Duong VB, Sahamitmongkol R, Tangtermsirikul S. Effect of leaching on carbonation resistance and steel corrosion of cement-based materials. Construction and Building Materials. 2013;40:1066-75.

[18] Somai M, Giri A, Roka A, Bhattarai J. Comparative studies on the anti-corrosive action of waterproofing agent and plant extract to steel rebar. Macromolecular Symposia. 2023;410(1):2100276.

[19] Amiri AS, Erdogmus E, Richter-Egger D. A comparison between ultrasonic guided wave leakage and half-cell potential methods in detection of corrosion in reinforced concrete decks. Signals. 2021;2:413-33.

[20] Yodsudjai W, Pattarakittam T. Factors influencing half-cell potential measurement and its relationship with corrosion level. Measurement: Journal of the International Measurement Confederation. 2017;104:159-68.

[21] Long X, Chen Z, Li P. Seismic performance of corroded ECC-GFRP spiral-confined reinforced-concrete column. Polymers. 2024;16(15):2110.

[22] Moussa AMA, Ibrahim AMA, Elsayed A, Wu Z, Monier A. Axial compression behavior of square RC columns confined by rectangular BFRP and hybrid ties. Infrastructures. 2025;10(8):206.

[23] Sahani K, Khadka SS, Sahani SK. Influence of corrosion on lifespan of reinforced concrete structures: a comprehensive review. Kathmandu University Journal of Science, Engineering and Technology. 2024;18(1):1-14.

[24] Liu Y, Hao H, Hao Y. Damage prediction of RC columns with various levels of corrosion deteriorations subjected to blast loading. Journal of Building Engineering. 2023;80:108019.

[25] Ali M, Shams MA, Bheel N, Almaliki AH, Mahmoud AS, Dodo YA, et al. A review on chloride induced corrosion in reinforced concrete structures: Lab and in situ investigation. RSC Advances. 2024;14(50):37252-71.

[26] Zhang R, Liu P, Ma L, Yang Z, Chen H, Zhu HX, et al. Research on the corrosion/permeability/frost resistance of concrete by experimental and microscopic mechanisms under different water–binder ratios. International Journal of Concrete Structures and Materials. 2020;14:10.

[27] Kaewunruen S, Wu L, Goto G, Najih YM. Vulnerability of structural concrete to extreme climate variances. Climate. 2018;6(2):40.

[28] Pan T. Continuous damage of concrete structures due to reinforcement corrosion: A micromechanical and multi-physics-based analysis. Journal of Building Engineering. 2024;95:110139.

[29] Elena C, Chiara P, Gianni B, Alessandra M. Corrosion attack in existing reinforced concrete structures: in-field investigation and analysis of naturally corroded bars. Materials and Structures. 2024;57:243.